Oceanologia (2020) 62, 173—189

Available online at www.sciencedirect.com

ScienceDirect

journal homepage: www.journals.elsevier.com/oceanologia

ORIGINAL RESEARCH ARTICLE

Simulating tropical storms in the Gulf of Mexico using analytical models

Mehdi Yaghoobi Kalourazi[1], **Seyed Mostafa Siadatmousavi**[1,*], **Abbas Yeganeh-Bakhtiary**[1], **Felix Jose**[2]

[1] *School of Civil Engineering, Iran University of Science and Technology, Narmak, Tehran, Iran*
[2] *Department of Marine & Earth Sciences, Florida Gulf Coast University, Fort Myers, FL, USA*

Received 12 June 2019; accepted 7 November 2019
Available online 25 November 2019

KEYWORDS
Analytical wind model;
H*Wind;
Buoy data;
Optimization;
Hurricanes;
Gulf of Mexico

SUMMARY Different analytical models have been evaluated for estimating wind speed of the tropical storm, where the storm-induced wind velocity is calculated as a function of distance from the center of the hurricane. For these models, different parameters such as maximum wind speed, a radius of the maximum wind, hurricane shape parameter, hurricane translation speed and the orientation of the trajectory, etc., affect the shape of a hurricane. Hurricanes Lili (2002), Ivan (2004), Katrina (2005), Gustav (2008) and Ike (2008) from the Gulf of Mexico were used for skill assessment. The maximum wind radius was calculated using significant wind radii (R_{34}, R_{50} and R_{64}) reported by the National Hurricane Center. Different formulas for calculating the radius of maximum wind speed were evaluated. The asymmetric wind field for each hurricane was generated using analytic methods and compared with in situ data from buoys in the Gulf of Mexico and the H*Wind data. Analytical models were able to predict high wind speed under tropical cyclone conditions with relatively high precision. Among the analytical models evaluated in this research, the model proposed by Holland et al. (2010) showed excellent results. Dynamical wind models such as NCEP/NARR provide wind speed with the coarse spatial resolution which is acceptable for far-field locations away from the hurricane eye. In contrast, analytical models were able to produce sufficiently reliable wind speed within a particular radius from the center of the hurricane. Therefore blending of dynamical and analytical models can be used to provide accurate wind data during hurricane passage in the Gulf of Mexico.

* Corresponding author at: School of Civil Engineering, Iran University of Science and Technology, Narmak, Tehran, Iran.
E-mail address: siadatmousavi@iust.ac.ir (S.M. Siadatmousavi).
Peer review under the responsibility of the Institute of Oceanology of the Polish Academy of Sciences.

Production and hosting by Elsevier

https://doi.org/10.1016/j.oceano.2019.11.001

1. Introduction

A tropical cyclone (TC) is a rapidly rotating storm system characterized by a low-pressure center and strong winds. TC might be called a hurricane, typhoon, tropical storm, tropical depression, or a cyclone depending on their intensity over different locations around the world. In general, a tropical cyclone generates high energy winds, incredible waves, torrential rain, and coastal flooding from storm surge. When it approaches the coast making landfall, the huge waves and storm surge are major threats to human life and property in coastal regions of the world. Among such susceptible coasts, one may refer to the northern Gulf of Mexico; where enormous property damage, and loss of life are ubiquitously associated with TC landfalls each year. As a result, simulation and prediction of tropical storms are of paramount importance.

Depperman (1947) adopted a model called Rankine vortex based on the rotation of the current around a rigid body to simulate the hurricane. This model was then modified by Hughes (1952) who presented the modified Rankine vortex model (MRV). Jelesniansky (1992) proposed a model called Sea, Lake, and Overland Surges from Hurricanes (SLOSH) for simulating hurricanes and its impact along the coast. Houston et al. (1999) evaluated the differences between Hurricane Research Division (HRD) surface wind analysis data and results of SLOSH model. There are several analytical relationships for modeling surface wind velocity of a hurricane, based on the radial distance from the hurricane center (e.g. DeMaria and Kaplan, 1994; Holland, 1980; Holland et al., 2010; Jelesniansky, 1967; Knaff et al., 2007; Willoughby et al., 2006; Wood et al., 2013). Considering Holland (1980) model and Advanced Coastal Circulation (ADCIRC) model for simulating a hurricane in the symmetrical and asymmetrical conditions, Mattocks and Forbes (2008) developed a deterministic prediction system for hurricanes and corresponding floods induced by storm surge along the North Carolina coast. The results led to National Weather Service (NWS) models such as NWS8 and NWS19, for simulating symmetrical and asymmetrical hurricanes in the Surface-Water Modeling Solution. Harper (2002), Atkinson and Holliday (1977), Dvorak (1975), Knaff and Zehr (2007), and Holland (2008) evaluated the relationships between the maximum wind velocity, V_{max}, and central pressure of the hurricane. In Holland (1980), the centeral pressure of the hurricane decreases with an increase in maximum sustained wind speed. Given the fact that the Holland (1980) method assumes a symmetric hurricane, while an actual hurricane is asymmetric in its core, recent studies improved the Holland (1980) model for asymmetric hurricane condition (e.g. Chen et al., 2003; Xie et al., 2006).

Several empirical formulations have been focused on calculating the maximum wind radius (R_{max}) in asymmetric conditions (e.g. Graham and Nunn, 1959; Kawai et al., 2005; Knaff et al., 2007; Takagi et al., 2012). Xie et al. (2006) employed the significant wind radii (R_{34}, R_{50} and R_{64}) at four quadrants of the hurricane to estimate R_{max}). Phadke et al. (2003) used existing analytical wind models to evaluate performance of the wind field resulted from Hurricane Iniki. Emanuel (2004) derived a model for the outer region of the hurricane, based on the combination of free-tropospheric thermodynamic balance and boundary-layer Ekman dynamic balance. He used angular entropy and the momentum balance in the boundary layer and for the inner convective region of the hurricane. In these solutions, the absolute temperature of the outflow is assumed nearly constant; whereas Emanuel and Rotunno (2011) showed this assumption is flawed in most of the cases. They argued that the thermal stratification of the outflow was set by small-scale turbulences which would limit the Richardson Number; implying the variation of outflow temperature with angular momentum. Such variation leads to a realistic prediction of the vortex structure of a hurricane.

Wind structure in a hurricane is based upon two components in the northern hemisphere: a counter-clockwise rotation of the surface background wind and the storm translation speed. Lin and Chavas (2012), and later Chavas et al. (2015) have mathematically merged existing theoretical solutions for the radial wind structure on the top of the boundary layer in the inner ascending region of the hurricane. It was based on the solution of Emanuel and Rotunno (2011) in which convective transfer of moisture and heat was persistent. In the outer descending region, the solution of Emanuel (2004) was employed in which the convection was absent. Hu et al. (2012) proposed a parametric hurricane wind model based on the asymmetric Holland-type vortex models. They included the impact of Coriolis deflection on the hurricane shape parameter. They also excluded the forward velocity of hurricane before applying the Holland vortex model to avoid unnecessary exaggeration of the wind asymmetry.

In general, analytical wind models are suitable for simulating wind field up to a specific radius from the center of hurricane, and beyond which prediction would go wrong as hurricane may be affected by other global weather systems. Wood et al. (2013) showed that central pressure deficit in an axisymmetric vortex core is strongly related to the choice of free parameters that control the shape of the radial profiles of the tangential velocity. A new model to represent TC wind velocity field is developed by Wijnands et al. (2016) consisting three components fit to the maximum wind velocities in the eye to capture the extent of gale-force winds around the TC, and the construction of the wind profile using a cubic spline approach.

Another method for simulating hurricane wind is to use long-term reanalysis wind data such as data provided by the National Centers for Environmental Prediction (NCEP), the European Centre for Medium-Range Weather Forecasts (ECMWF), and the Cross-Calibrated Multi-Platform (CCMP). Such wind data have also been extensively used for

hindcasting and predicting the hydrodynamics in various ocean basins. However, studies have shown that the use of such coarse-resolution reanalyzed data for forcing wave models led to underestimation of wave height. The quality of wind data is always blamed for such an underestimation (e.g. Brenner et al., 2007; Cavaleri and Sclavo, 2006; Mazaheri et al., 2013; Moeini et al., 2010; Signell et al., 2005). Combining two data sources, i.e., Holland (1980) model and CCMP data, Pan et al. (2016) reported improvement in wind field hindcast for two TCs, i.e., Fanapi and Meranti, which made landfall in China. They evaluated the effect of different TC models on hindcasting V_{max}. Combining wind data from different sources have been used extensively for improving hurricane wave modeling in the Gulf of Mexico (e.g. SiadatMousavi et al., 2009).

This study quantitatively evaluates the wind fields calculated using different parametric models for several hurricanes traversed across the Gulf of Mexico. Given that R_{max} is an important parameter contributing to the storm-induced wind velocity, its influences on the wind field is compared among different analytic methods and the most appropriate method is selected for calculating R_{max} in the Gulf of Mexico. All evaluations were based on in situ data from National Data Buoy Center (NDBC) buoys. Finally, most appropriate analytical model data were compared against H*Wind model in terms of hurricane forward motion, angle of the maximum wind velocity, V_{max} and the range in which analytical model is applicable. The results of analytical models were also compared with NCEP/NARR (North American Regional Reanalysis) dynamical model to determine whether it is possible to merge both datasets to produce an optimized wind data for the study area.

2. Parametric tropical storm-induced wind velocity

Wind vector, V, of a TC is composed of rotational velocity of the hurricane and the translational motion of the hurricane eye, and can be expressed as follows:

$$V = k_m V_r + \delta_m V_m, \tag{1}$$

where V_r is velocity over a distance r from the hurricane center, V_m is the hurricane translation velocity, k_m can be considered as 0.8 according to Powell (1980); however, his later observational studies (e.g. Powell et al., 1991, 1998) have showed its variability over the range 0.7 to 0.9, due to variations in the vertical stability. The asymmetry coefficient δ_m is equal to zero for a symmetric hurricane and 0.5 for an asymmetric one.

Numerous methods have been proposed for calculating V_r. Schloemer (1954) proposed a radial relationship for calculating the pressure based on the difference between the central surface pressure of the hurricane (P_c) and the ambient pressure (P_n). Later on, Holland (1980, hereafter H80) modified the Schloemer's theory and presented a rectangular hyperbola radial relationship between pressure and wind velocity as follows:

$$P(r,\theta) = P_c + (P_n - P_c)\exp\left[\left(-\frac{R_{\max(\theta)}}{r}\right)\right]^B, \tag{2}$$

$$V_r(r,\theta) = \left[\frac{B}{\rho_a}\left(\frac{R_{\max(\theta)}}{r}\right)^B (P_n - P_c)\exp\left[\left(-\frac{R_{\max(\theta)}}{r}\right)\right]^B + \left(\frac{rf}{2}\right)^2\right]^{0.5} - \frac{rf}{2}, \tag{3}$$

where ρ_a is the density of air, $P(r, \theta)$ is the surface pressure at a distance of r from the hurricane center, B is a hurricane shape parameter, f is the Coriolis parameter $f = 2\Omega\sin(\phi)$, Ω is the rotational frequency of the earth and φ is the latitude. The parameter "B" is used to relate the pressure to the wind field and it plays an important role in estimating V_{max} in a hurricane. Indeed, B controls the hurricane eye diameter and fastness of the maximum wind velocity, and varies from 1 to 2.5. It has been shown that B has high correlation with several parameters, such as pressure drop, R_{max}, and the latitude of hurricane center; e.g., the following relationship can be used to calculate hurricane aspect ratio (Levinson et al., 2010):

$$B = \frac{V_{max}^2 \rho_a e}{100(P_n - P_c)}, \tag{4}$$

where e is the base of natural logarithms.

Jelesniansky (1967) suggested a parametric equation to calculate V_r. This formula led to development of the US Weather Service SPALASH storm surge prediction model (Jelesnianski et al., 1973) and the SLOSH model (Jelesnianski, 1992, hereafter S92) as the following relationship:

$$V_r = \begin{cases} V_{max}\left(\frac{r}{R_{max}}\right)^{\frac{3}{2}}, & r < R_{max} \\ V_{max}\left(\frac{2\,R_{max} r}{r^2 + R_{max}^2}\right), & r \geq R_{max} \end{cases}. \tag{5}$$

Willoughby et al. (2006, hereafter W06) divided the hurricane structure into three parts such that the wind velocity inside the eye of a hurricane increases with increasing the radius from the center. Far from the hurricane eye, it decreases exponentially. A transition area exists between those mentioned areas. On this basis, the wind velocity in each part can be calculated from the following relationships.

$$V_r = \begin{cases} V_i = V_{max}\left(\frac{r}{R_{max}}\right)^n, & r < R_1 \\ V_i(1-w) + V_o, & R_1 \leq r < R_2 \\ V_o = V_{max}\left(-\frac{r - R_{max}}{X_1}\right), & r \geq R_2 \end{cases}, \tag{6}$$

where V_i and V_o are the tangential wind component in the eye and beyond the transition zone, which lies between $r = R_1$ and $r = R_2$; and permits velocity of V_{max} at the distance of R_{max}; X_1 is the exponential decay length in the outer vortex and n is the exponent for the power law inside the eye; w is the weighted function in the transitional zone. The values of R_{max}, X_1 and n are suggested as a function of V_{max} and φ, using the regression analysis:

$$\begin{cases} R_{max} = 46.4\exp(-0.0155V_{max} + 0.016\phi) \\ X_1 = 270.5 - 4.78V_{max} + 6.17\phi \\ n = 0.431 + 0.136V_{max} - 0.006\phi \end{cases}. \tag{7}$$

The weight function, w, is expressed based on the non-dimensional ξ which is defined as follows:

$$\xi = \frac{r - R_1}{R_2 - R_1}, \tag{8}$$

$$w(\xi) = \begin{cases} 0, & \xi \le 0 \\ 126\xi^5 - 420\xi^6 + 540\xi^7 - 315\xi^8 + 70\xi^9, & 0 \le \xi \le 1. \\ 1, & \xi \ge 1 \end{cases} \tag{9}$$

Knaff et al. (2007, hereafter K07) used MRV model as well as a statistical-parametric model to predict TC wind radii in the Atlantic Ocean, the East Pacific, and the Western North Pacific. They proposed a parametric equation to calculate V_r as follows:

$$V(r,\theta) = \begin{cases} (V_{max} - a)\left(\frac{R_{max}}{r}\right)^x + a\cos(\theta - \theta_0), & r \ge R_{max} \\ (V_{max} - a)\left(\frac{R_{max}}{r}\right) + a\sin(\theta - \theta_0), & r < R_{max} \end{cases} \tag{10}$$

in which x is the size parameter, a is the asymmetry coefficient, and θ_0 is the angle between V_{max} and the storm translation vector. In this equation, using the wind radii (R_{34}, R_{50} and R_{64}) in each quadrant and multiple linear regressions, four parameters (V_{max} , R_{max}, a, θ) can be calculated.

Holland et al. (2010, hereafter H10) retained the rectangular hyperbolic form of previously proposed H80 model and further refined wind velocity relationship at all levels and matched the wind velocity with the data beyond the rotational part of the hurricane. The proposed relationship in H10 is as follows:

$$\left[\frac{b_s}{\rho_a}\left(\frac{R_{\max(\theta)}}{r}\right)^{b_s}(P_n - P_c)\exp\left[\left(-\frac{R_{\max(\theta)}}{r}\right)\right]^{b_s} + \left(\frac{rf}{2}\right)^2\right]^x - \frac{rf}{2}, \tag{11}$$

where the subscript s refers to the surface value (at a nominal height of 10 m). Parameter b_s is the hurricane shape coefficient which can be related to the original b value in H80 by $b_s = bg_s^x$, where g_s is the reduction factor for gradient to-surface wind. If $x = 0.5$ is set, and b_s is assumed to be a constant value, as used in H80, then:

$$\begin{cases} b_s = -4.4 \times 10^{-5}\Delta P^2 + 0.01\Delta P + 0.03\frac{\partial P_c}{\partial t} \\ \quad - 0.014\phi + 0.15\, V_m + 1.0\phi \\ x = 0.6\left(1 - \frac{\Delta P}{215}\right) \end{cases}, \tag{12}$$

where $\Delta P = P_n - P_c$ is in hPa and $\partial P_c/\partial t$ is the rate of change of pressure in hPa/h. Emanuel and Rotunno (2011) extended the Emanuel (2004) model to areas beyond the hurricane eyewall by considering a constant (critical) Richardson Number which is determined based on temperature gradient across the hurricane. This model (hereafter E11) performs well near R_{max}, while becomes less accurate as one gets farther from the center of the hurricane. This model takes into account the Coriolis effect and may turn into Jelesnianski model upon ignoring those effects. E11 suggested the following model for simulating wind surface velocity in a TC:

$$V_r = \frac{2r\left(R_{max}V_{max} + \frac{1}{2}fR_{max}^2\right)}{R_{max}^2 + r^2} - \frac{fr}{2}. \tag{13}$$

Wood et al. (2013, hereafter W13) improved the existing parametric tangential wind profile model of Wood and White (2011) for a better fit to a TC. W13 model has five key parameters controlling the radial profile of tangential wind: V_{max}, R_{max}, and three shape velocity parameters η, λ and κ to control different portions of the profile:

$$\begin{cases} V_r(\rho; m) = V_{max}\phi(\rho; \kappa; \eta; \lambda) \\ \phi(\rho; \kappa; \eta; \lambda) = \frac{\eta^\kappa \rho^\lambda}{\left(\eta - \kappa + \kappa\rho^{\frac{\eta}{\lambda}}\right)^\lambda}, \end{cases} \tag{14}$$

where $\rho = r/R_{max}$ is a dimensionless radius. Note that $0 \le \kappa < \eta$ and $\lambda > 0$.

As discussed in this section, host of models have been proposed to simulate the wind structure of a TC. These formulations will be assessed in the following sections for understanding the complex structure of hurricane wind field in the Gulf of Mexico.

2.1. The radius of the maximum wind

The radius of the maximum wind refers to the distance from the center of the hurricane to the location within its structure where V_{max} occurs. R_{max} plays a significant role in hurricane characteristics. Numerous relationships have been proposed for calculating R_{max} in the literature. In this respect, Graham and Nunn (1959, hereafter G59) suggested Eq. (15) in which R_{max} is a function of latitude, difference between the central surface pressure and the ambient pressure, and translation speed of the tropical storm.

$$R_{max} = 28.25\tanh[0.0873(\phi - 28)] + 12.22\exp\left(\frac{\Delta P}{33.86}\right) + 0.2\, V_m + 37.2. \tag{15}$$

Kawai et al. (2005, hereafter K05) have proposed exponential formulas for R_{max} (km) based on the central pressure:

$$R_{max} = 94.89\exp\left(\frac{P_c - 967}{61.5}\right). \tag{16}$$

K07 suggested the following relationship where m_0, m_1, and m_2 are empirical parameters:

$$R_{max} = m_0 + m_1V_m + m_2(\phi - 25). \tag{17}$$

Takagi et al. (2012, hereafter T12) used the following empirical formula developed by the National Institute for Land and Infrastructure Management (NILIM) to estimate the R_{max}:

$$R_{max} = 80 - 0.769(950 - P_c), \tag{18}$$

where R_{max} and P_c are in km and hPa respectively, and $P_c < 950$ hPa.

Note that the National Hurricane Center (NHC) forecast advisories and the Automated Tropical Cyclone Forecasting (ATCF) product provide parameters such as geographic coordinates of hurricane center, V_{max}, V_m, surface wind forecasts etc., and the hurricane structure is provided by the radii of specified wind velocities (34, 50, 64, and 100 kn) in four quadrants. Figure 1 illustrates the asymmetric wind structure for Hurricane Ivan at 0900 UTC on 15 September 2004. At this time, the center of hurricane was located at 26.1°N, 87.8°W. The 1-min averaged maximum sustained

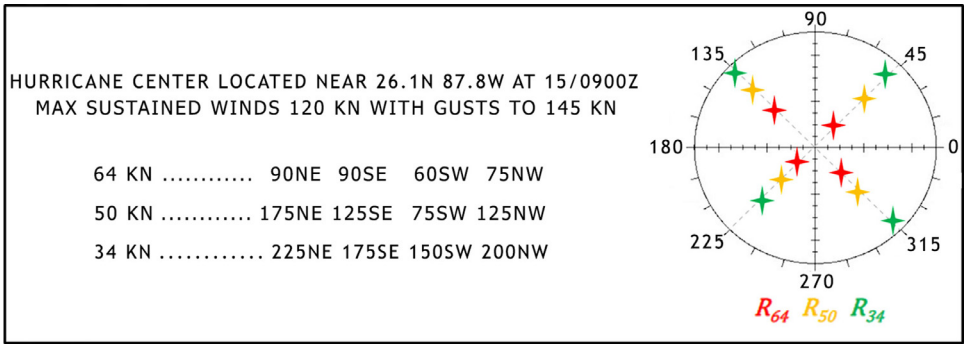

Figure 1 Tropical cyclone parameters provided by the National Hurricane Center (NHC) for Hurricane Ivan at 0900 UTC 09/15/2004.

surface wind speed was 120 kn with gusts up to 145 kn. The 64 kn wind in four quadrants (NE, SE, SW, NW) was located at distances of (90, 90, 60, 75 NM) from the center of the hurricane; Similar information is also provided for the location of 34 and 50 kn winds. Those distances in different quarters are shown as R_{34}, R_{50} and R_{64}. As proposed by Xie et al. (2006, hereafter X06), R_{max} can be set to different values in each quadrant. By solving Eq. (3), based on given information in each direction, curve fitting provides two solutions for R_{max} where the smaller value is the most appropriate solution. Details are presented in the Appendix 1.

3. Methodology

3.1. Selecting tropical storms for analyzing wind field in the Gulf of Mexico

The major hurricanes in the Gulf of Mexico during 2002–2016 include: Lili (2002), Ivan (2004), Katrina (2005), Alberto (2006), Dolly (2008), Gustav (2008), Ike (2008), Ida (2009), Alex (2010), Don (2011), Isaac (2012), Karen (2013) and Colin (2016). Due to non-availability of R_{64} values for some of the TCs, Hurricanes Lili, Ivan, Katrina, Gustav and Ike were selected for detailed study of their complex wind structure. The time period from the entry of tropical storms into the Gulf of Mexico until its landfall along northern Gulf coast was considered for each hurricane. The best hurricane track, geographic coordinates, central pressure, V_{max}, V_m, etc. were retrieved on a six-hourly basis from NHC and ATCF. Moreover, for model validation purpose, corresponding wind data have been extracted from NDBC buoy network from the Gulf of Mexico. The hurricane tracks and available buoys are shown in Figure 2.

3.2. Reconstructing the wind fields of a tropical storm

In order to estimate wind field using analytical models, polar coordinate system was employed. In this study, radius, r, was calculated from 1 to 1000 by steps of 1 km and started from the hurricane center. The azimuthal angle from x-axis, θ, was considered from 1° to 360° by steps of 1°.

4. Results and discussions

4.1. Effect of hurricane shape parameter (B) on the tropical storm-generated wind field

As it was mentioned in section 2, hurricane shape parameter (B) serves as a control parameter for the hurricane shape. It establishes a balance between V_{max} and P_c. H80 proposed a range from 1 to 2.5 for B. In this section the effect of B on wind velocity and the hurricane shape was investigated. In Figure 3, the wind fields of Hurricane Ivan on 15 September 2004, at 0900 UTC was demonstrated for different values of B (0.5–2.5). In this case, $V_{max} = 120$ kn $= 61.73$ m/s, $R_{max} = 40.21$ km and $P_c = 932$ hPa, and the wind velocity was calculated using H80's model. Increasing B would also increase V_{max} at R_{max} and decrease the wind speed away from R_{max}. In case of $B = 1.5$, the corresponding wind velocity at $R_{max} = 40.21$ km was ~60 m/s, indicating that the most appropriate value for B at this instance is ~1.5. It is in agreement with actual hurricane conditions reported by NHC in Figure 1.

4.2. Assessment of different models for calculating R_{max}

Different analytical models such as G59, K05, X06, K07 and T12 can be employed to calculate R_{max}, and the key question is, which method is consistent for the hurricanes traversing across the Gulf of Mexico. In order to address this question, the values of R_{max} calculated using different models and R_{max} derived from H*Wind are compared in Figure 4 for the time interval when Hurricane Ivan was churning across the Gulf of Mexico; i.e. from 1500 UTC on 14 September 2004 to 0300 UTC 16 September 2004. H*Wind is a product of NOAA/Hurricane Research Division which integrates data from all available surface weather platforms and aircraft data within 1000 km from hurricane's eye. The root mean square error (RMSE), scattering index (SI) and BIAS presented in Figure 4 were used to assess the models. It can be concluded that T12, K07 and K05 methods tend to overestimate R_{max} throughout the time period when the Hurricane was active in the Gulf of Mexico until it leaves the Gulf of Mexico. In fact, according to Eq. (16) and Eq. (18), R_{max} in the K05 and T12 methods only depends on P_c which provides limited flexibility to produce realistic values. In contrast, R_{max} in the G59

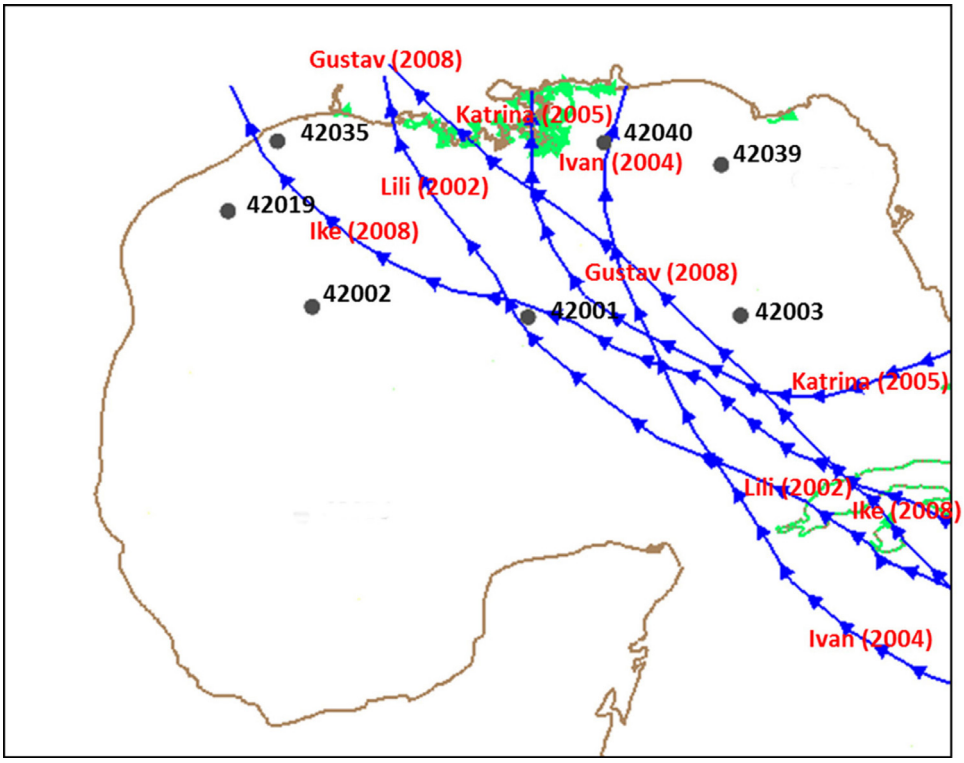

Figure 2 Tracks of five major hurricanes that made landfall along the northern Gulf of Mexico and locations of National Data Buoy Center (NDBC) buoys used for models assessment in the study.

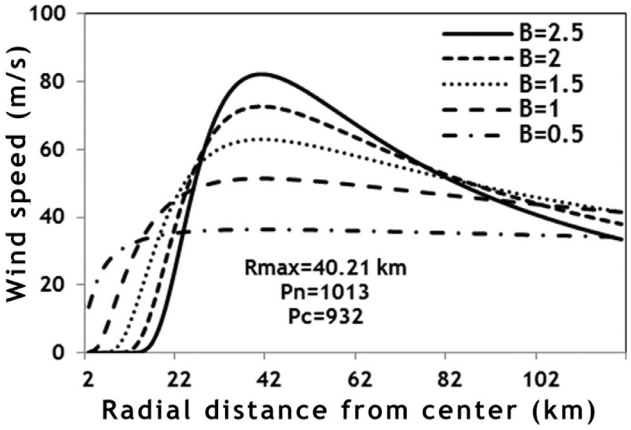

Figure 3 The effect of varying the parameter B on wind velocity for Hurricane Ivan at 0900 UTC 09/15/2004.

and X06 methods is also dependent on the V_m and the geographical location of the tropical cyclone. Therefore, these methods give more desirable results for calculating R_{max}. Based on the statistics presented in Figure 4, X06 was the most successful method in reproducing R_{max}.

4.3. Assessment of different parametric models for calculating the wind field of a tropical storm

Different models can be used to simulate a tropical storm in the Gulf of Mexico including H80, S92, W06, K07, H10, E11 and W13 models as presented in section 2. In all of these models, R_{max} serves as a key parameter, and the formula proposed by X06 was selected as the most appropriate method for calculating R_{max} in the Gulf of Mexico as shown in section 4.2. For assessment, the wind velocities calculated via the analytical approaches were compared to the measured data from NDBC buoys.

4.3.1. Hurricane Lili

Hurricane Lili was one of the strongest hurricanes passing through large areas across the Atlantic Ocean and the Gulf of Mexico and made its landfall along the northern Gulf of Mexico on October 4th, 2002. Comparison between the model-generated wind velocity using H80, S92, W06, K07, H10, E11 and W13 models and the measured data from buoys in the Gulf of Mexico are illustrated in Figure 5. In general, the storm-induced wind velocity was maximum at $r = R_{max}$ while lower velocities were observed in both $r < R_{max}$ (inside the hurricane eyewall) and $r > R_{max}$ (far from the hurricane center). According to Figure 2, this hurricane passed near buoy 42001 on October 2nd when $R_{max} = \sim$23 km and the radial distance between the buoy and the hurricane center $r = \sim$27 km. Since $r \approx R_{max}$, the buoy 42001 was expected to measure V_{max}. As shown in Figure 5, there is a fair agreement between measured data at all buoys and the analytical models.

In order to evaluate the analytical models in more detail, some statistics were presented in Table 1. The BIAS values indicate that, almost all models tend to underestimate the wind velocity at most of the buoys locations. Based on statistics, H10 and W13 models produced better results at most of the buoys compared to other models.

A comparison of wind structure generated by symmetric and asymmetric models for Hurricane Lili at 2100 UTC

Table 1 Statistical parameters characterizng wind velocity obtained using different parametric methods at buoys locations in the Gulf of Mexico during different hurricanes.

Hurricane Lili (2002)

	NDBC-42001							NDBC-42002							NDBC-42003						
	H80	S92	W06	K07	H10	E11	W13	H80	S92	W06	K07	H10	E11	W13	H80	S92	W06	K07	H10	E11	W13
RMSE (m/s)	2.7	3.9	3.0	2.8	2.4	3.6	2.6	2.4	3.1	2.1	2.9	2.0	2.9	1.8	1.9	3.5	3.4	2.2	1.6	3.0	1.5
SI (%)	15	15	20	15	15	18	13	38	32	37	20	33	37	28	18	18	30	14	15	19	12
BIAS (m/s)	−1.5	−3.2	−0.8	1.1	−1.1	−2.4	1.8	−1.3	−2.6	1.0	1.6	−1.0	−2.2	1.0	0.4	−2.9	−1.3	−1.7	0.2	−2.2	0.7

Hurricane Ivan (2004)

	NDBC-42001							NDBC-42002							NDBC-42003						
	H80	S92	W05	K07	H10	E11	W13	H80	S92	W05	K07	H10	E11	W13	H80	S92	W05	K07	H10	E11	W13
RMSE (m/s)	2.2	2.9	3.3	3.7	2.3	3.7	2.9	2.7	1.7	2.5	1.5	2.5	1.4	1.6	2.6	2.9	1.8	2.8	2.6	2.6	1.6
SI (%)	17	19	17	24	19	24	19	44	41	39	41	46	37	38	9	10	8	7	8	10	5
BIAS (m/s)	1.4	−1.4	0.4	−0.6	−0.2	−2.8	−1.3	2.2	0.8	−2.0	1.4	2.0	−0.3	0.9	0.9	−2.0	−0.6	−1.6	2.0	−1.6	1.1

Hurricane Katrina (2005)

	NDBC-42001							NDBC-42002							NDBC-42019						
	H80	S92	W06	K07	H10	E11	W13	H80	S92	W06	K07	H10	E11	W13	H80	S92	W06	K07	H10	E11	W13
RMSE (m/s)	2.3	4.5	3.4	3.8	3.1	5.2	3.1	1.5	2.6	4.1	2.4	2.1	3.0	1.8	2.0	1.7	2.1	2.3	1.8	2.0	2.1
SI (%)	17	27	27	22	32	27	24	27	38	35	25	36	37	30	39	39	47	41	37	43	42
BIAS (m/s)	−0.8	−2.6	−1.5	−0.9	−1.3	−3.1	−1.3	0.3	−1.0	−2.0	−1.2	−0.2	−1.3	−0.1	1.0	0.4	0.5	−1.0	1.1	0.1	1.2

Hurricane Gustav (2008)

	NDBC-42001							NDBC-42019							NDBC-42040						
	H80	S92	W06	K07	H10	E11	W13	H80	S92	W06	K07	H10	E11	W13	H80	S92	W06	K07	H10	E11	W13
RMSE (m/s)	3.3	7.6	2.3	3.1	3.3	7.0	3.4	2.4	3.4	2.3	2.2	1.5	3.8	1.8	3.4	5.7	3.4	2.2	2.8	7.0	2.2
SI (%)	25	20	18	15	21	19	17	37	13	27	13	13	18	15	22	13	21	12	10	13	13
BIAS (m/s)	−1.6	−7.2	−0.8	−2.1	−2.2	−6.6	−2.1	−0.5	−3.3	−1.4	−1.2	−1.2	−3.7	−1.5	0.2	−5.3	−0.8	−1.3	−2.2	−6.7	1.1

Hurricane Ike (2008)

	NDBC-42002							NDBC-42019							NDBC-42040						
	H80	S92	W06	K07	H10	E11	W13	H80	S92	W06	K07	H10	E11	W13	H80	S92	W06	K07	H10	E11	W13
RMSE (m/s)	2.6	3.9	3.6	3.8	2.3	3.3	3.0	2.7	4.1	3.8	3.1	1.7	4.5	2.2	2.9	4.0	3.8	3.2	1.5	4.0	2.9
SI (%)	18	21	28	24	12	27	26	24	12	22	30	17	15	21	20	11	22	26	11	11	20
BIAS (m/s)	1.6	−2.9	−2.2	−1.6	−1.5	−0.3	0.3	1.4	−2.8	−3.1	−0.4	−0.5	−3.0	−0.3	1.7	−2.9	−1.2	−1.5	−0.4	−2.9	−0.9

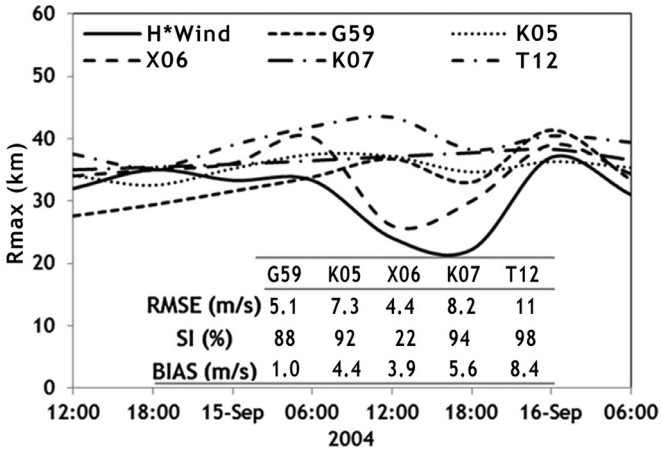

Figure 4 Comparison of the performance of different models applied for calculating R_{max} for Hurricane Ivan (2004).

on 01 October 2002 is provided in Figure 6. The amount of asymmetry depends on V_{max}, R_{max}, V_m and the direction of the hurricane movement (β). The center of hurricane was located near 22.7°N, 85°W at this time, and $V_{max} = 90$ kn, $\beta = 305°$, $V_m = 15$ kn, $P_C = 970$ hPa. Since W13 and H10 methods produced higher wind velocity compared to other models, their corresponding asymmetric structure for the hurricanes are also higher. Increasing the asymmetric amount affect the θ_{max} (the angle of maximum wind velocity). According to the direction of the hurricane movement, the wind surface velocity on the right side of the hurricane is larger than the left side.

4.3.2. Hurricane Ivan

Hurricane Ivan, the strongest hurricane during the 2004 Atlantic hurricane season, resulted in a widespread damage in the Caribbean and United States, and reached Category 5 strength on the Saffir-Simpson scale. It passed across the Gulf of Mexico during 14–16 September. It is evident from Figure 2 that Hurricane Ivan trajectory passed close to buoys 42001, 42003 and 42040. Since wind velocity is higher on the right of the hurricane rather than its left side, higher wind velocity was measured at buoy 42003 than the buoys 42001 on September 15th (see Figure 5). A comparison between the results of parametric models and the measured wind velocity data by buoys shows that the models performances were better during peak hours.

Statistical indices based on data from different buoys presented in Table 1 indicate that E11 underestimated the wind velocity; while H80 tended to overestimate the wind velocity at most of the buoys. The RMSE values at all buoy locations show that all analytical models provided fairly realistic estimation of Hurricane Ivan. In general, H80, H10 and W13 models outperformed the rest of models, especially close to high speed regions of the hurricane. Figure 6 illustrates the wind field simulated by the symmetric and asymmetric models for Hurricane Ivan at 0900 UTC on 15 September 2004. At this time, the hurricane center was located at 26.1°N, 87.8°W, and $V_{max} = 120$ kn, $\beta = 340°$, $V_m = 10$ kn, $P_C = 938$ hPa. Among the analytical models, the wind field and the wind field asymmetry were maximum for H10 model. As an example, at the same radial distances from hurricane center and in the direction of θ_{max}, higher surface wind velocities were estimated by H80 and H10 models and the smallest wind speeds were simulated by S92 and E11. Table 2 illustrates a comparison between wind radii (R_{34}, R_{50} and R_{64}) reported by NHC and H80, H10, E11 models for Hurricane Ivan at 0900 UTC on 15 September 2004. There is relatively good agreement between NHC report and analytical models in terms of the shape of hurricane and the values of wind surface velocity; however, H80 and H10 models overestimated the wind radius, while the E11 underestimated the wind radius.

4.3.3. Hurricane Katrina

Hurricane Katrina was one of the most destructive natural disasters occurred in the United States during the last decades. The hurricane landfall occurred on August 29th along the Mississippi coast as an upper Category 3 Hurricane. As shown in Figure 2, the buoys 42001, 42003 and 42040 were close to the hurricane track. A comparison between the analytical models and measured data in Figure 5 reveals that the performance of analytical models were acceptable; however, the performance was better at buoys 42001 and 42040, compared to other buoys. It can be inferred that the analytical models tend to estimate wind velocity more accurately close to the area of maximum wind speed of a hurricane.

4.3.4. Hurricane Gustav

Hurricane Gustav caused serious destruction in parts of Haiti, the Dominican Republic, Jamaica, the Cayman Islands, Cuba and the United States. As shown in Figure 2, the buoys 42003, 42039 and 42040 were located on the right flank of the hurricane track. The eyeball observation of results presented in Figure 5 and the statistical indices presented in Table 1 show that in most of the buoy locations wind velocity was underestimated by all models. Moreover, K07, H10 and W13 models produced more realistic results when compared to other parametric models for simulating the Hurricane Gustav.

4.3.5. Hurricane Ike

Hurricane Ike entered the Gulf of Mexico during 10–13 September 2008 and passed close to the buoy 42001 on

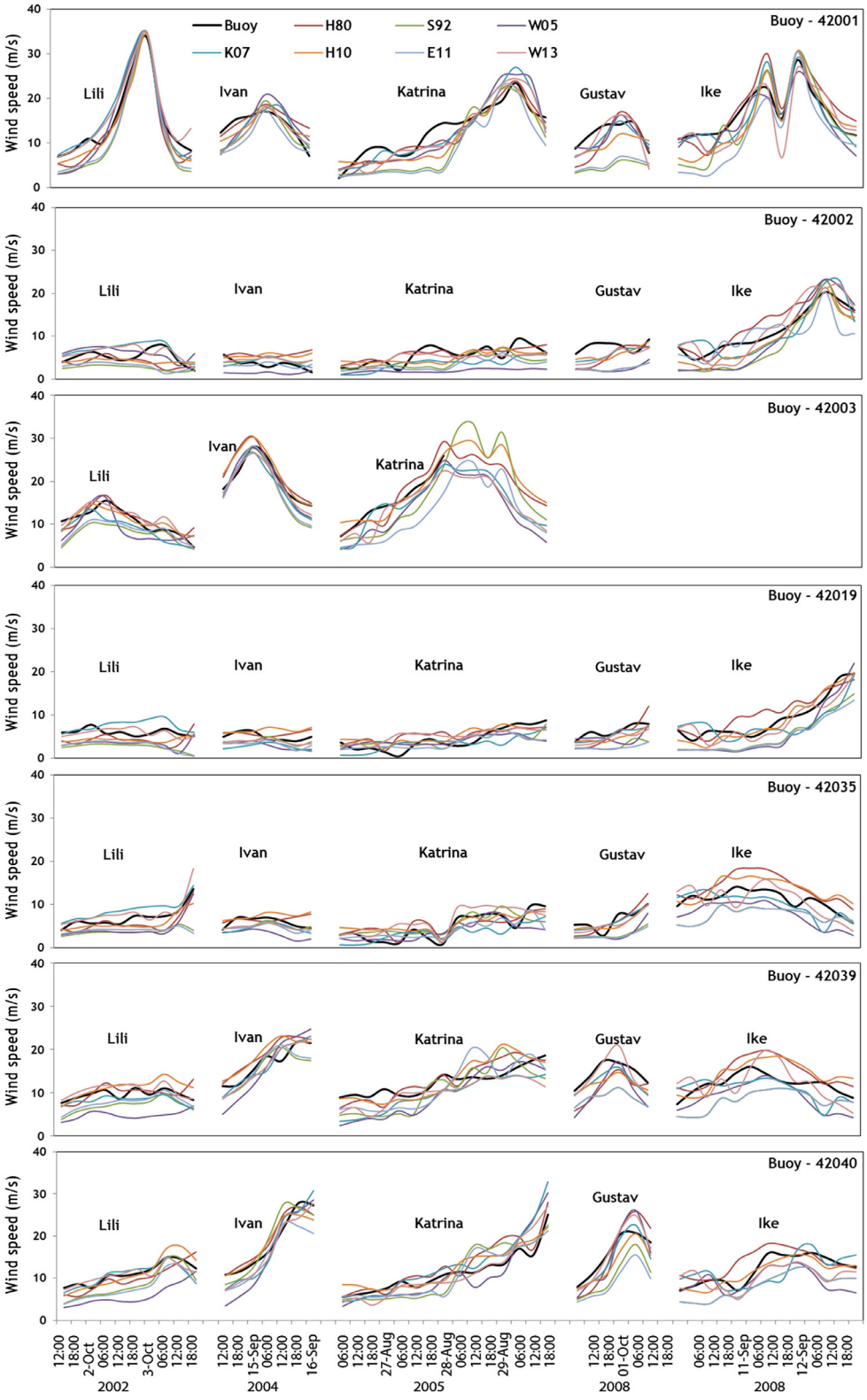

Figure 5 Performance of different methods applied for calculating wind velocity as compared to buoys wind velocity measurements in the Gulf of Mexico during Hurricanes Lili, Ivan, Katrina, Gustav and Ike.

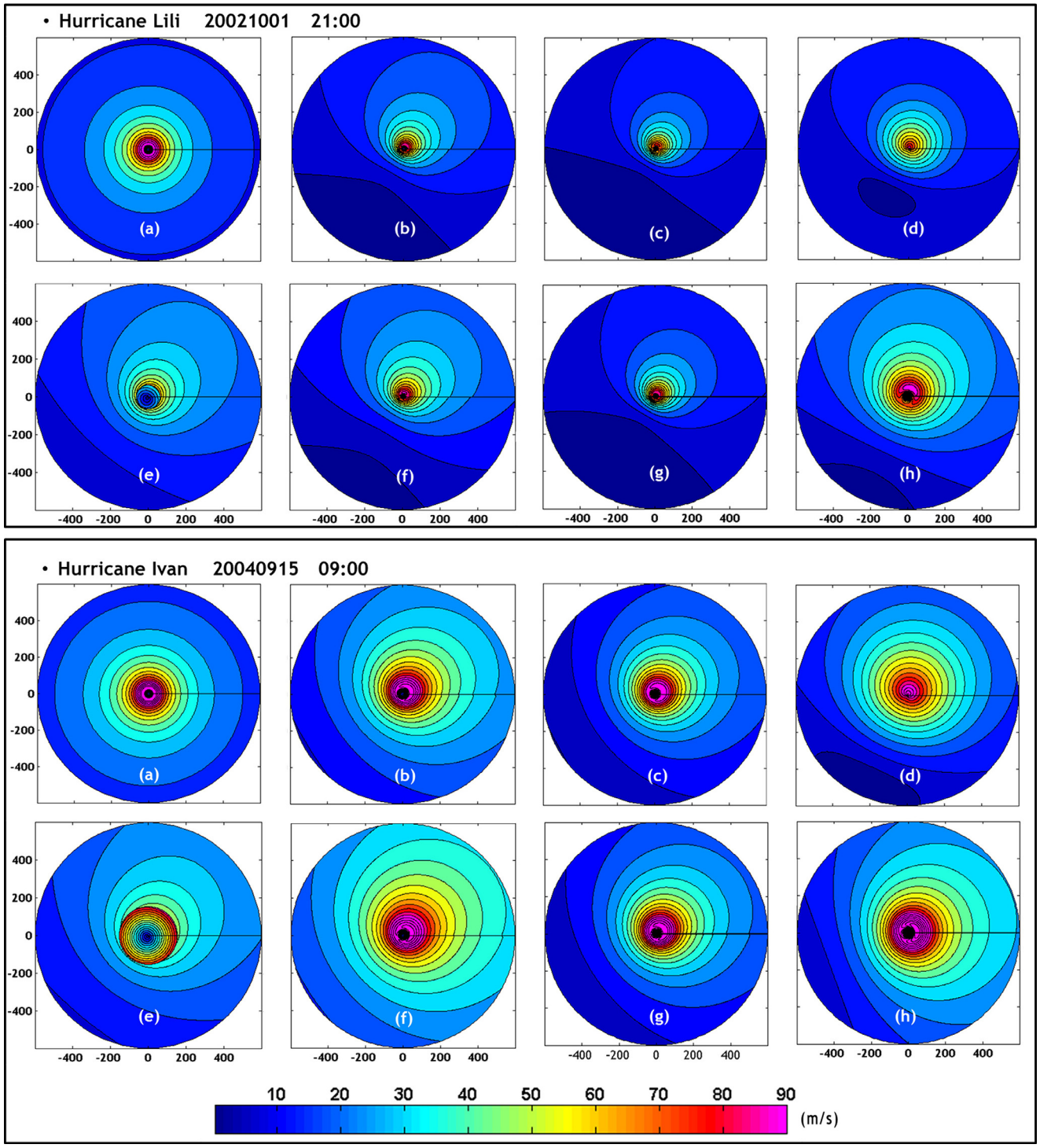

Figure 6 Comparison of the wind fields produced by (a) symmetric, (b) H80, (c) S92, (d) W06, (e) K07, (f) H10, (g) E11, (h) W13, models for the Hurricane Lili at 21:00 10/01/2002 and for the Hurricane Ivan at 09:00 09/15/2004 in the Gulf of Mexico.

September 11th when $R_{max} = \sim 25$ km and the radial distance of the buoy from the center of hurricane was calculated as $r = \sim 5$ km. The storm-induced wind velocity at this buoy, as shown in Figure 5, reduced suddenly when buoy was inside the eye ($r \ll R_{max}$). As summarized in Table 1, S92, W06, K07 and E11 models underestimated the wind velocity at most of the buoys locations. The models proposed by H10 and W13 showed better performance for simulating the Hurricane Ike compared to other analytical models.

4.3.6. Calibrating k_m to improve models' performance

As discussed in the previous section, among different analytical models, the models proposed by S92, W06, K07, and E11 relatively underestimated the wind velocity, while those proposed by H80, H10 and W13 tend to overesti-

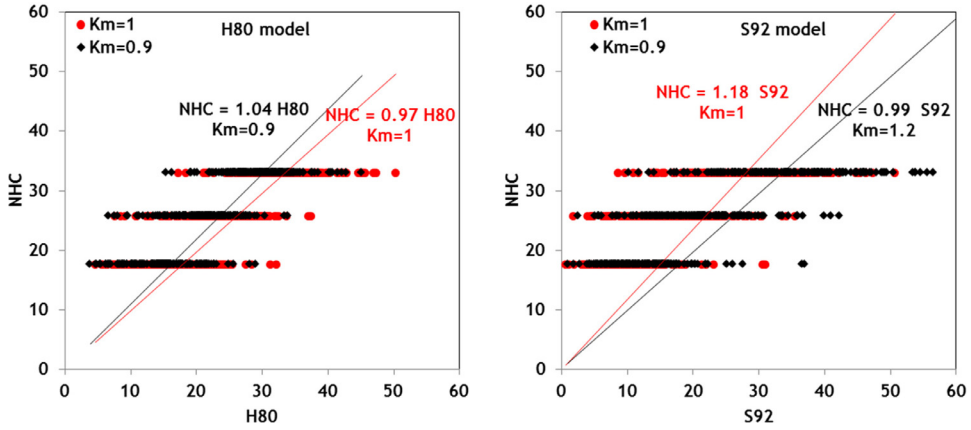

Figure 7 Scatter plot and linear regression of wind velocities (m/s) produced by NHC versus H80 (left panel) and S92 (right panel) models for all tracks of the Hurricanes Lili, Ivan, Katrina, Gustav and Ike.

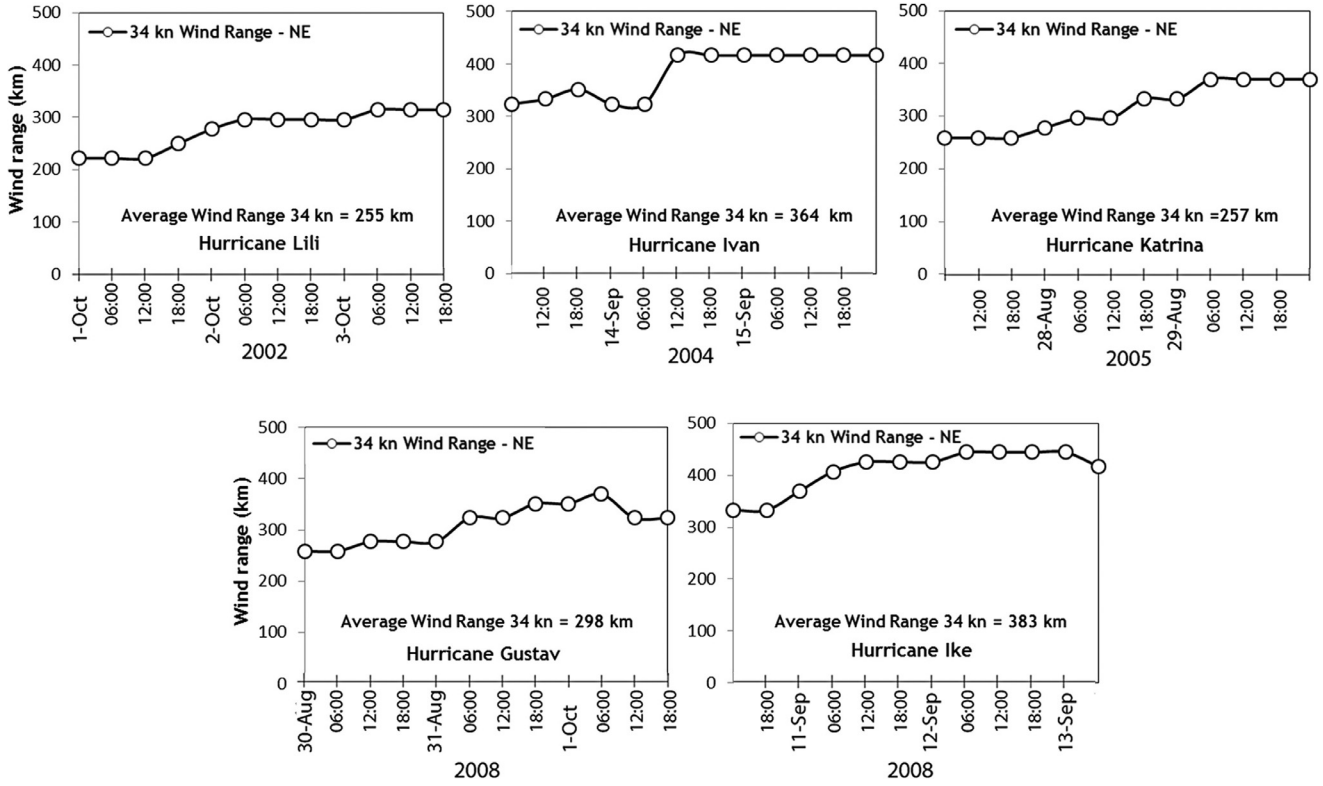

Figure 8 Values of R_{34} produced by NHC for the northeast quarter in 12 snapshots during the Hurricanes Lili, Ivan, Katrina, Gustav and Ike passage over the Gulf of Mexico.

Table 2 Comparison between wind radii (R_{34}, R_{50} and R_{64}) reported by NHC and obtained using H80, H10, E11 models for Hurricane Ivan at 09:00 09/15/2004.

	NHC				H80				H10				E11			
	NE	SE	SW	NW	NE	SE	SW	NW	NE	SE	SW	NW	NE	SE	SW	NW
64 kn	90	90	60	75	96	68	50	76	122	85	61	94	89	71	48	65
50 kn	175	125	75	125	139	95	69	110	184	121	89	146	122	96	63	86
34 kn	225	175	150	200	244	122	109	191	303	213	143	272	182	142	88	122

mate the storm-induced wind velocity. It is possible to calibrate hurricane models by adjusting k_m in Eq. (1) which is 0.7 ~ 0.9 by default (Powell et al., 1991, 1998). Along the track of each hurricane 12 points were selected, and the R_{34}, R_{50} and R_{64} in four quadrants (NE, SE, SW, and NW) reported by NHC were used in models to estimate the wind speed. These estimates from analytical relations were compared with NHC reported speeds (34, 50 and 64 kn) for all aforementioned hurricanes. Figure 7 provides the scatter plots for the H80 and S92 models. To calculate the calibration coefficient, $k_m = 1$ were used in all models and the linear regression provided the ratio of wind velocity between NHC and each analytical model. As shown in Figure 7, the ratio was equal to 0.97 and 1.18 for the H80 and S92 models, respectively. It means that S92 requires k_m value higher than 1 in Eq. (1) while vice versa is true for the H80 model. By trial and error process, $k_m = 1.2$ and $k_m = 0.9$ were found suitable for S92 and H80 models. Similarly, using a linear regression for other analytical models, the values of k_m for each model were estimated as presented Table 3. The BIAS values presented in Table 3 show the improvement of models in reproducing wind velocities at NDBC buoys when calibrated values of k_m were used in analytical models.

4.4. Combining parametric models with numerical models

A comparison between analytical models and observed data from NDBC buoys shows that these models produce relatively appropriate wind velocity within a particular radius to the center of hurricane (R_{he} = radius of the hurricane effect), and the accuracy of simulations degrade as one gets beyond that threshold radius. The *SI* and *RMSE* values were lower at buoys within shorter distance to the hurricane track (i.e. close to R_{max}), as compared to those located farther from the track. R_{he} value depends on R_{max}, V_{max}, and P_c; which may differ for different hurricanes. Since high wind speeds are more important in hurricane modeling, and the fact that the least reported speed by NHC is 34 kn, it is wise to assume that the maximum of R_{he} can be equal to ~R_{34}. Values of R_{34} in 12 snapshots of the Hurricanes Lili, Ivan, Katrina, Gustav and Ike are illustrated in Figure 8. As an example, for Hurricane Ivan, the values of R_{34} varied from 300 to 400 km; hence R_{he} in Hurricane Ivan can be selected as 400 km. With an average of R_{34} from all snapshots, it is possible to determine R_{he} for each hurricane. The values of R_{he} for the Hurricanes Lili, Ivan, Katrina, Gustav and Ike during the time period that these hurricanes were active in the Gulf of Mexico are selected as 300, 400, 350, 350 and 450 km. The Hurricanes Ivan and Ike have the largest range of effect, while hurricanes Lili and Gustav have the least impacted range in the Gulf of Mexico.

In Figure 9, the wind speeds extracted from NCEP/NARR and H*Wind at certain times for different hurricanes were compared with wind speeds calculated by the H10 model. NCEP/NARR is an atmospheric dynamical model which employs regional data for assimilation.

Resolution of wind data for NCEP/NARR, H*Wind and analytical models are 0.3°, 0.0542° and 0.01° respectively (an arbitrary value for the analytical model used here). NCEP/NARR was less accurate than H*Wind data and analytical models during high speeds, most likely due to its

Table 3 Bias values corresponding to different k_m values in analytical models at locations of buoys in the Gulf of Mexico during all hurricanes.

	NDBC-All buoys – Hurricane Lili						NDBC-All buoys – Hurricane Ivan						NDBC-All buoys – Hurricane Katrina					
	H80	S92	W06	K07	H10	E11	W13	H80	S92	W06	K07	H10	E11	W13	H80	S92	W06	K07	H10	E11	W13
k_m	1.0	1.0	1.0	1.0	1.0	1.0	1.0	1.0	1.0	1.0	1.0	1.0	1.0	1.0	1.0	1.0	1.0	1.0	1.0	1.0	1.0
BIAS (m/s)	1.1	−3.7	−3.4	−1.2	0.9	−3.3	1.8	2.2	−1.2	−2.8	−1.6	2.5	−2.3	1.2	1.3	−2.7	−2.5	−2.3	0.8	−3.3	0.6
Calibrated k_m	0.9	1.2	1.2	1.2	0.9	1.2	0.9	0.9	1.2	1.2	1.2	0.9	1.2	0.9	0.9	1.2	1.2	1.2	0.9	1.2	0.9
BIAS	−0.6	−2.8	−2.5	0.4	−0.3	−2.4	0.9	1.2	−0.6	−1.7	−1.0	1.3	−1.6	−0.1	0.4	−1.5	−1.4	−1.2	0.02	−2.0	−0.5
	NDBC-All buoys – Hurricane Ike							NDBC-All buoys – Hurricane Gustav													
	H80	S92	W06	K07	H10	E11	W13	H80	S92	W06	K07	H10	E11	W13							
k_m	1.0	1.0	1.0	1.0	1.0	1.0	1.0	1.0	1.0	1.0	1.0	1.0	1.0	1.0							
BIAS	3.6	−3.9	−3.5	−2.1	0.8	−4.1	0.6	−1.4	−6.2	−4.3	−3.1	−1.4	−6.5	−0.4							
Calibrated k_m	0.9	1.2	1.2	1.2	0.9	1.2	0.9	0.9	1.2	1.2	1.2	0.9	1.2	0.9							
BIAS (m/s)	2.2	−2.6	−2.0	−0.9	−0.2	−2.7	−0.1	−1.7	−4.9	−3.0	−1.6	−1.7	−5.1	−1.2							

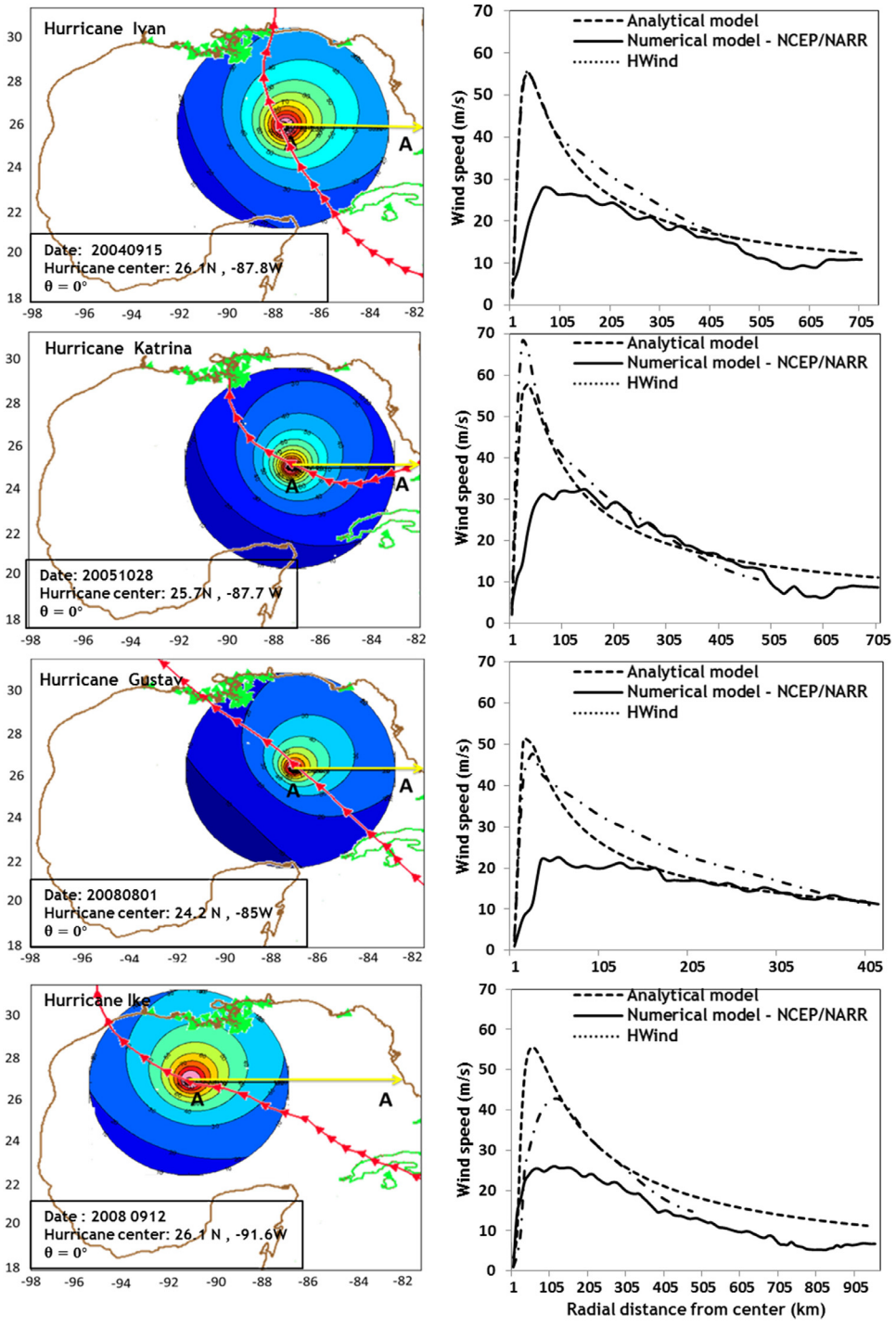

Figure 9 Comparison of the wind velocities produced by the analytical model (H10), numerical model (NCEP/NARR) and H*Wind during at 09/15/2004 (Hurricane Ivan), 10/25/2005 (Hurricane Katrina), 08/31/2008 (Hurricane Gustav) and 09/12/2008 (Hurricane Ike).

coarser spatial resolution; e.g. the V_{max} of H10 and H*Wind for Hurricane Ivan at 0900 UTC 15 September 2004 was 120 kn and 116 kn while corresponding value from NCEP/NARR was 100 kn. Therefore, NCEP/NARR data are not suitable close to R_{max}. There is also a fair agreement between calibrated H10 model and high resolution H*Wind data. Note that H*Wind data are available up to a radius of 480 km from the center of the hurricane, which is roughly equivalent to the value of R_{he}. This figure shows that when the high quality wind field is desired during a hurricane passage, e.g. for a wave simulation, one might adopt an analytical relationship or H*Wind from the center of hurricane up to $r = R_{he}$, and blend it with wind velocity values from model simulations such as *NCEP/NARR* or *ECMWF* database when $r > R_{he}$ to capture the effect of wind dynamics close to the hurricane center.

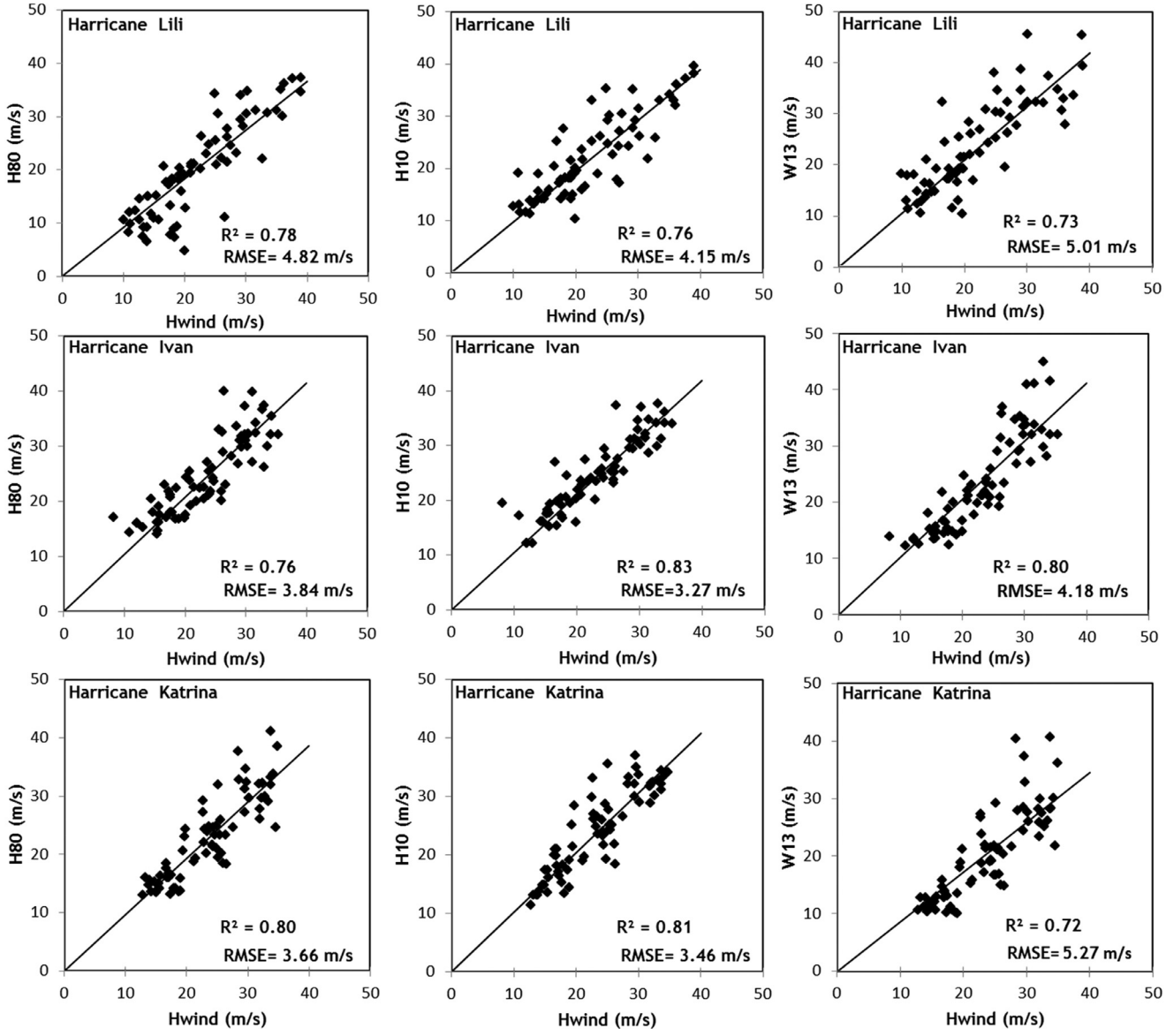

Figure 10 Scatter plot of wind velocities produced by H*Wind versus H80, H10 and W13 models for 12 points along the tracks of Hurricanes Lili, Ivan and Katrina.

4.5. Assessment of analytical models using H*Wind data

H*Wind is one of the most reliable data to describe the wind structure during tropical storm. Atlantic Oceanographic and Meteorological Laboratory combines all surface wind data measured from sea, land, and air (using by either a satellite or an airplane) during the course of a hurricane to produce H*Wind. A moving box with the center located at the center of the hurricane and side length of 2°, 4°, or 8° can be extracted including storm-induced wind velocity data with spatial resolution of 0.0542° and temporal resolution of at least six-hour (Powell and Houston, 1998; Powell et al., 1998). In section 4.3, it has been shown that the analytical models H80, H10 and W13 can better simulate the tropical storm-induced wind field in the Gulf of Mexico compared to other analytical models. To select the most appropriate analytical models in the Gulf of Mexico, the simulated wind speed data from the models H80, H10 and W13 were compared with the H*Wind data. For this purpose, 12 points along the track of each hurricane were selected in four quadrants (NE, SE, SW, NW). Then, wind velocities at different wind radii were extracted from H*Wind corresponding to each point from the center of the hurricane, and compared to wind speed predicted by analytical models. Scatter plots including coefficient of determination (R^2) and RMSE for the Hurricanes Lili, Ivan and Katrina are shown in Figure 10. There is a good agreement between the results of the analytical models and H*Wind model for all hurricanes; however the H10 model outperforms other models when compared to the H*Wind data. For instance, in the case of Hurricane Ivan, RMSE values for H80, H10 and W13 models were 3.84, 3.27 and 4.18 m/s and R^2 values were 0.76, 0.83 and 0.83, respectively.

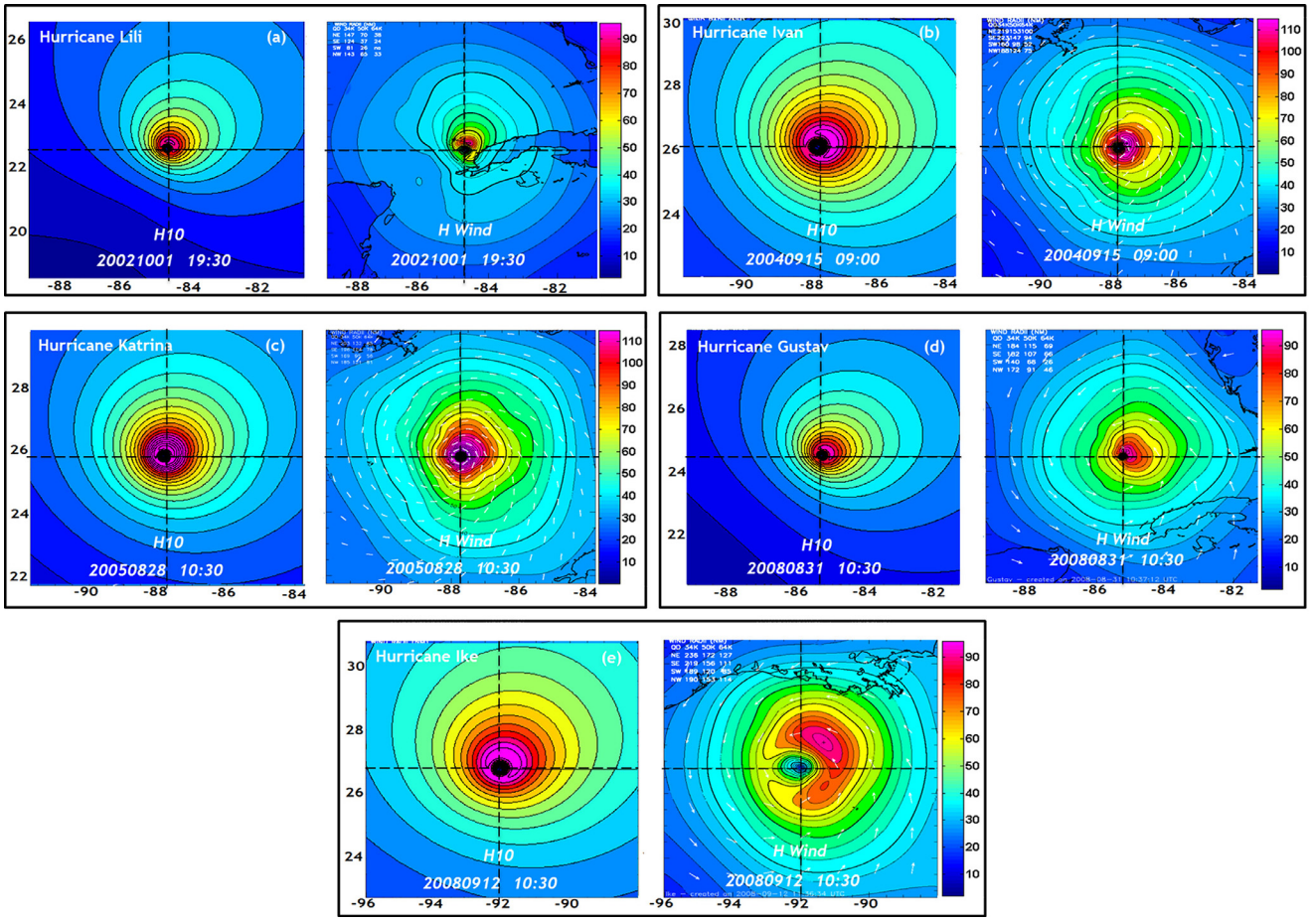

Figure 11 Comparisons of H*Wind distributions and H10 model wind fields during (a) Hurricane Lili at 19:30 UTC, 10/01/2002 (b) Hurricane Ivan at 09:00 UTC, 09/15/2004 (c) Hurricane Katrina at 12:00 UTC, 10/28/2005 (d) Hurricane Gustav at 10:30 UTC, 08/31/2008 (e) Hurricane Ike at 10:30 UTC, 09/12/2008.

Figure 11 displays surface wind fields computed using H10 model as the most appropriate analytical models when compared to H*Wind during different hurricanes. Note that analytical models such as H10 are calibrated based on NHC observed data at four points across the hurricane at limited number of radii (R_{34}, R_{50} and R_{64}), while the H*Wind model is developed based on data measured across the entire hurricane. Hence, a more detailed shape of a hurricane is expected from H*Wind model rather than from parametric models such as H10. A fair agreement was observed between results of H10 model and those of H*Wind model in all hurricanes. In general, for locations across the hurricane, where $r > R_{max}$, the wind velocity obtained from H*Wind model was higher than that estimated by H10 model. V_{max} is one of the most important parameters when comparing an analytical model like H10 to the H*Wind model. Table 4 shows the values of V_{max} were close for both methods during different hurricanes.

Table 4 Comparison of the maximum wind velocity produced by H*Wind and H10 model at times shown in Figure 11.

Hurricane	Model	V_{max} (kn)
Hurricane	H*Wind	94
Lili	H10	92
Hurricane	H*Wind	116
Ivan	H10	115
Hurricane	H*Wind	139
Katrina	H10	138
Hurricane	H*Wind	99
Gustav	H10	96
Hurricane	H*Wind	92
Ike	H10	98

5. Conclusions

Hurricane-generated wind field in the Gulf of Mexico was simulated using a series of analytical models. The B parameter and R_{max} are considered as control parameters for simulating a hurricane; and as a first step, the different methods for determining R_{max} have been compared to determine the most appropriate model for the region. Seven different analytical models, viz., H80, S92, W06, K07, H10,

E11 and W13 have been assessed based on buoys' observations and H*Wind data. The important findings of this research are summarized as follows:

- Increasing B would also increase V_{max} at R_{max} and decrease the wind speed away from R_{max}; hence, at every instant along a hurricane track and having distinct P_c, V_{max} and R_{max}, there is a unique value for B parameter, which provides a more realistic illustration of the wind field in the hurricane. Note that H80 proposed 1 to 2.5 as an acceptable range for B parameter.
- Five analytical models including G59, K05, X06, K07 and T12 were evaluated to calculate R_{max}. Among these methods, the X06 formulation provided the best performance when compared with H*Wind data. Therefore, X06 method is recommended for calculating R_{max} in the Gulf of Mexico.
- Comparison between the results of analytical models and the observed wind velocity data at seven buoy locations across Gulf of Mexico showed that there is a fair agreement between the analytical models and observed data. The models proposed by S92, W06, K07, and E11 relatively underestimated the wind velocity, while those proposed by H80, H10 and W13 slightly overestimated the storm-induced wind velocity. The linear regression was used between NHC and analytical data to calibrate k_m coefficient in the analytical model (see Eq. (1)). Hence, the value of k_m can be set to 1.2 in S92, W06, K07, E11 methods and 0.9 in H80, H10 and W13 methods, respectively.
- The results presented in this study suggested that the H10 model outperformed other methods in estimating wind field in the Gulf of Mexico.
- Comparison between analytical models with H*Wind data revealed that analytical models are able to produce sufficiently reliable wind velocity within a particular radius from the center of the hurricane (R_{he}). Based on the results of this study, R_{he} is estimated between 300 and 450 km.
- Dynamic wind models such as NCEP/NARR are not suitable for calculating high wind speeds close to hurricane eye due to their relatively coarse spatial resolution. On the other hand, the accuracy of the wind field estimated by analytical models degrades beyond R_{he}. Therefore, one might adopt an analytical model or H*Wind from the center of hurricane up to R_{he}, and blend it with wind velocities from dynamic models such as NCEP/NARR for $r > R_{he}$.
- It was found that there is a very good agreement between the results of the wind fields from the H10 and the H*Wind data. However; it underestimates the wind velocity when $r \gg R_{max}$.

Appendix 1: Algorithm to calculate the radius of the maximum wind

It was stated that R_{max} is the most important parameter affecting the results of analytical models. The stronger a hurricane, the larger its maximum wind radius will be. As stated in section 4.2, the method proposed by X06 is selected as a base for calculating R_{max} in this study. Note that Eq. (3) can be decomposed into two parts y_1 and y_2 as follows:

$$\begin{cases} y_1 = \left(V_r + \frac{rf}{2}\right)^2 - \frac{\rho_a}{B(P_n - P_c)}\left(\frac{rf}{2}\right)^2 \\ y_2 = \left(\frac{R_{\max(\theta)}}{r}\right)^B \exp\left[\left(-\frac{R_{\max(\theta)}}{r}\right)\right]^B \end{cases}. \quad (18)$$

In the above equations, the term $(y_1 - y_2)^2$ would be minimized at a particular R_{max} for each pair of r and V_r in dataset. Substituting the values of 34, 50, 64 kn as V_r (1 kn = 0.5144 m/s) and R_{34}, R_{50} and R_{64} as r (1 nm = 1.85 km), the R_{max} can be obtained in each of the four quadrants of the hurricane. For example, the R_{max} values computed at four quadrants in Hurricane Ivan at 0900 UTC 15 September 2004 were 47.12, 38.72, 28.65 and 43.67 n mi for NE, SE, SW and NW. These values should be interpolated to determine R_{max} at any point around the center of the hurricane. Following X06, a polynomial function was used (see Eq. (19)). The R_{max} values at angles of 45°, 135°, 225° and 335°, and the condition of R_{max} (0) = R_{max} (360) can be used to determine the coefficients ($i = 1–5$, Pi)

$$R_{max}(\theta) = P_1\theta^{n-1} + P_2\theta^{n-2} + \ldots + P_{n-1}\theta + P_n. \quad (19)$$

References

Atkinson, G.D., Holliday, C.R., 1977. Tropical cyclone minimum sea level pressure/maximum sustained wind relationship for the western North Pacific. Mon. Weather Rev. 105, 421–427.

Brenner, S., Gertman, I., Murashkovsky, A., 2007. Preoperational ocean forecasting in the southeastern Mediterranean Sea: Implementation and evaluation of the models and selection of the atmospheric forcing. Mar. Sys. 65, 268–287.

Cavaleri, L., Sclavo, M., 2006. The calibration of wind and wave model data in the Mediterranean Sea. Coast. Eng. 53, 613–627.

Chavas, D.R., Lin, N., Emanuel, K., 2015. A model for the complete radial structure of the tropical cyclone wind field. Part I: Comparison with observed structure. J. Atmos. Sci. 72, 3647–3662.

Chen, Y., Brunet, G., Yau, M., 2003. Spiral bands in a simulated hurricane. Part II: Wave activity diagnostics. J. Atmos. Sci 60, 1239–1256.

DeMaria, M., Kaplan, J., 1994. A statistical hurricane intensity prediction scheme (SHIPS) for the Atlantic basin. Weather Forecast 9, 209–220.

Depperman, R.C.E., 1947. Notes on the origin and structures of Philippine typhoons. B. Am. Meteorol. Soc. 28, 399–404.

Dvorak, V.F., 1975. Tropical cyclone intensity analysis and forecasting from satellite imagery. Mon. Weather Rev. 103, 420–430.

Emanuel, K. , 2004. Tropical cyclone energetics and structure. In: Fedorovich, E., Rotunno, R., Stevens, B. (Eds.), Atmospheric Turbulence and Mesoscale Meteorology 165–192.

Emanuel, K., Rotunno, R., 2011. Self-Stratification of Tropical Cyclone Outflow. Part I: Implications for Storm Structure. J. Atmos. Sci. 68, 2236–2249.

Graham, H.E., Nunn, D.E. , 1959. Meteorological Considerations Pertinent to. Standard Project Hurricane, Atlantic and Gulf Coasts of the United States. Weather Bureau, U.S. Department of Commerce, Washington, D.C., 317 pp.

Harper, B., 2002. Tropical cyclone parameter estimation in the Australian region: wind pressure relationships and related issues for engineering planning and design, Rep. no. J0106-PR003E, Woodside Energy, Ltd., 92 pp.

Holland, G., 2008. A revised hurricane pressure—wind model. Mon. Weather Rev. 136, 3432—3445.
Holland, G.J., 1980. An analytic model of the wind and pressure profiles in hurricanes. Mon. Weather Rev. 108, 1212—1218.
Holland, G.J., Belanger, J.I., Fritz, A., 2010. A revised model for radial profiles of hurricane winds. Mon. Weather Rev. 138, 4393—4401.
Houston, S.H., Shaffer, W.A., Powell, M.D., Chen, J., 1999. Comparisons of HRD and SLOSH surface wind fields in hurricanes: Implications for storm surge modeling. Weather Forecast 14, 671—686.
Hu, K., Chen, Q., Kimball, S.K., 2012. Consistency in hurricane surface wind forecasting: an improved parametric model. Nat. Hazards 61, 1029—1050.
Hughes, A.L., 1952. On the low level wind structure of tropical cyclones. J. Meteaor. 9, 422—428.
Jelesnianski, C.P., Taylor, A.D., 1973. A preliminary view of storm surges before and after storm modifications. In: Environmental Research Laboratories. Weather Modification Program Office, Boulder, C.O., p. 33.
Jelesniansky, C.P., 1967. Numerical Computations of Storm Surges With Bottom Stress. Mon. Weather Rev. 95, 740—756.
Jelesniansky, C.P., 1992. SLOSH: Sea, lake, and overland surges from hurricanes. NOAA Technical Rep. NWS 48, US Dept. Commerce, NOAA, NWS, Alice Springs MD, 73 pp.
Kawai, H., Honda, K., Tomita, T., Kakinuma, T., 2005. Characteristic of Typhoons in 2004 and Forecasting and Hindcasting of Their Storm Surges. Tech. Note Port and Airport Res. Inst., No 1103, 34 pp.
Knaff, J.A., Sampson, C.R., DeMaria, M., Marchok, T.P., Gross, J.M., McAdie, C.J., 2007. Statistical tropical cyclone wind radii prediction using climatology and persistence. Weather Forecast 22, 781—791.
Knaff, J.A., Zehr, R.M., 2007. Reexamination of tropical cyclone wind—pressure relationships. Weather Forecast 22, 71—88.
Levinson, D., Vickery, P., Resio, D., 2010. A review of the climatological characteristics of landfalling Gulf hurricanes for wind, wave, and surge hazard estimation. Ocean Engin. 37, 13—25.
Lin, N., Chavas, D., 2012. On hurricane parametric wind and applications in storm surge modeling. J. Geophys. Res.-Atmos. 117, art. no D09120, 19 pp., https://doi.org/10.1029/2011JD017126.
Mattocks, C., Forbes, C., 2008. A real-time, event-triggered storm surge forecasting system for the state of North Carolina. Ocean Model 25, 95—119.
Mazaheri, S., Kamranzad, B., Hajivalie, F., 2013. Modification of 32 years ECMWF wind field using QuikSCAT data for wave hindcasting in Iranian Seas. J. Coast. Res. 65, 344—350.
Moeini, M., Etemad-Shahidi, A., Chegini, V., 2010. Wave modeling and extreme value analysis off the northern coast of the Persian Gulf. Appl. Ocean Res. 32, 209—218.
Pan, Y., Chen, Y.-P., Li, J.-X., Ding, X.-l., 2016. Improvement of wind field hindcasts for tropical cyclones. Water Sci. Eng. 9, 58—66.
Phadke, A.C., Martino, C.D., Cheung, K.F., Houston, S.H., 2003. Modeling of tropical cyclone winds and waves for emergency management. Ocean Eng. 30, 553—578.
Powell, M.D., 1980. Evaluations of diagnostic marine boundary-layer models applied to hurricanes. Mon. Weather Rev. 108, 757—766.
Powell, M.D., Dodge, P.P., Black, M.L., 1991. The landfall of Hurricane Hugo in the Carolinas: Surface wind distribution. Weather Forecast 6, 379—399.
Powell, M.D., Houston, S.H., 1998. Surface wind fields of 1995 hurricanes Erin, Opal, Luis, Marilyn, and Roxanne at landfall. Mon. Weather Rev. 126, 1259—1273.
Powell, M.D., Houston, S.H., Amat, L.R., Morisseau-Leroy, N., 1998. The HRD real-time hurricane wind analysis system. J. Wind Eng. Industrial Aerodynam. 77—78, 53—64.
Schloemer, R.W., 1954. Analysis and synthesis of hurricane wind patterns over Lake Okeechobee, Florida. Hydrometeorological Rep. 31, Department of Commerce and U.S. Army Corps of Engineers, U.S. Weather Bureau, Washington, DC, 49 pp.
Siadatmousavi, S., Jose, F., Stone, G., 2009. Simulating Hurricane Gustav and Ike wave fields along the Louisiana inner shelf: Implementation of an unstructured third-generation wave model, SWAN. In: Proc. Oceans 2009 Conf., 873—880.
Signell, R.P., Carniel, S., Cavaleri, L., Chiggiato, J., Doyle, J.D., Pullen, J., Sclavo, M., 2005. Assessment of wind quality for oceanographic modelling in semi-enclosed basins. J. Mar. Syst. 53, 217—233.
Takagi, H., Nguyen, D., Esteban, M., Tran, T., Knaepen, H.L., Mikami, T., 2012. Vulnerability of coastal areas in Southern Vietnam against tropical cyclones and storm surges. In: The 4th International Conference on Estuaries and Coasts (ICEC2012), 8 pp.
Wijnands, J.S., Qian, G., Kuleshov, Y., 2016. Spline-based modelling of near-surface wind speeds in tropical cyclones. Appl. Math. Model. 40, 8685—8707.
Willoughby, H., Darling, R., Rahn, M., 2006. Parametric representation of the primary hurricane vortex. Part II: A new family of sectionally continuous profiles. Mon. Weather Rev. 134, 1102—1120.
Wood, V.T., White, L.W., 2011. A new parametric model of vortex tangential-wind profiles: Development, testing, and verification. J. Atmos. Sci. 68, 990—1006.
Wood, V.T., White, L.W., Willoughby, H.E., Jorgensen, D.P., 2013. A new parametric tropical cyclone tangential wind profile model. Mon. Weather Rev. 141, 1884—1909.
Xie, L., Bao, S., Pietrafesa, L.J., Foley, K., Fuentes, M., 2006. A real-time hurricane surface wind forecasting model: Formulation and verification. Mon. Weather Rev. 134, 1355—1370.